ROYAL SOCIETY
OF CHEMISTRY

View Article Online
View Journal | View Issue

Check for updates

Enhanced Fe(II)/Fe(III) cycle by boron enabled efficient Cr(VI) removal with microscale zero-valent iron

Wenjuan Shen, [ID] [a] Yan Gao,[a] Zhan Liu,[a] Xu Zhang,[b] Fengjiao Quan,*[a] Xing Peng,*[b] Xiaobing Wang,[c] Jianfen Li,[a] Zhenhua Qin,[a] Yun He[a] and Hui Li[a]

Recently, researchers have been paying much attention to zero-valent iron (ZVI) in the field of pollution remediation. However, the depressed electron transport from the iron reservoir to the iron oxide shell limited the wide application of ZVI. This study was aimed at promoting the performance of microscale ZVI (mZVI) for hexavalent chromium (Cr(VI)) removal by accelerating iron cycle with the addition of boron powder. It was found that the addition of boron powder enhanced the Cr(VI) removal rate by 2.1 times, and the proportion of Cr(III) generation after Cr(VI) removal process also increased, suggesting that boron could promote the reduction pathway of Cr(VI) to Cr(III). By further comparing the Cr(VI) removal percentage of Fe(III) with or without the boron powder, we found that boron powder could promote the percentage removal of Cr(VI) with Fe(III) from 10.1% to 33.6%. Moreover, the presence of boron powder could decrease the potential gap values (ΔE_p) between Fe(III) reduction and Fe(II) oxidation from 0.668 V to 0.556 V, further indicating that the added boron powder could act as an electron sacrificial agent to promote the reduction process of Fe(III) to Fe(II), and thus enhancing the reduction of Cr(VI) with Fe(II). This study shed light on the promoted mechanism of Cr(VI) removal with boron powder and provided an environmentally friendly and efficient approach to enhance the reactivity of the mZVI powder, which would benefit the wide application of mZVI technology in the environmental remediation field.

1. Introduction

Recently, due to the characteristics of low cost, high abundance, and environmental benignity, ZVI is being developed to be a compelling solution to tackle environmental pollution problems, including advanced oxidation of organic pollutants, nutrient removal, heavy metal control, groundwater, and soil remediation.[1–9] In general, ZVI possesses a typical core–shell structure, including an iron core serving as an electron reservoir toward heavy metal reduction, and an iron oxide shell containing ample active complexation sites for heavy metal ions.[10] However, the heavy metal removal efficiency is unsatisfactory due to the ineffective electron transport from the iron core to the iron oxide shell. Therefore, considerable efforts are being devoted to accelerating the electron flow or selectivity. Zhang *et al.* developed oxyanion-modified ZVIs, such as phosphate-modified nZVI, phosphorylated nZVI, oxalate-modified ZVI,

oxalated mZVI, and strained-mZVI with interstitial boron doping, aiming at promoting the decontamination performance and utilization efficiency.[11–14] Moreover, as electrons released from the iron reservoir are greatly dependent on the strength of the lattice Fe–Fe interactions, strategies are being designed to develop amorphous ZVI with longer Fe–Fe bond distance.[15] Additionally, a number of physical or chemical measures, including ultrasound, weak magnetic field, sulfidation, ball-milling, and noble metal doping, were also put forward to improve the activity of ZVI.[16–19]

Actually, these approaches toward ZVI reactivity improvement in many scenarios were based on the promotion of ZVI corrosion by enhancing the ferrous or ferric ions dissolution, and the accelerated iron dissolution process would facilitate the heavy metal reduction or flocculation. Actually, regulating the iron cycle process during ZVI application and improving the utilization efficiency of ferrous ions can also be an effective method to improve the efficiency of ZVI toward pollutant removal. In recent years, there have been reports that boron crystals could significantly speed up the Fe(III)/Fe(II) cycle in a Fenton-like reaction for the degradation of pollutants.[20] Furthermore, boron was demonstrated to be active for Fe(II) regeneration in Fenton-like peroxydisulfate and peracetic acid activation.[21,22] Moreover, many boron-containing compounds

[a]School of Chemical and Environmental Engineering, Wuhan Polytechnic University, Wuhan, 430023, P. R. China. E-mail: fjquan@ccnu.edu.cn

[b]Key Laboratory of Pesticide & Chemical Biology of Ministry of Education, Institute of Environmental & Applied Chemistry, Central China Normal University, Wuhan 430079, P. R. China. E-mail: pengxing185@163.com

[c]School of Chemistry and Civil Engineering, Shaoguan University, Shaoguan, 512023, P. R. China

were also developed to improve the efficiency of the iron cycle.[23–29]

In the periodic table, the specific electronic configuration ($1s^2 2s^2 2p^1$) of the metalloid element boron usually endows boron with high affinity to the metalloid and metal elements. Boron atoms with low valency on the surface of boron powder could provide electrons for $Fe(III)$ species to generate $Fe(II)$.[21] As the reduction of some heavy metals relies on the electron transport from the inner iron core and the released ferrous ions, it is reasonable to assume that boron could also enable the performance of ZVI for heavy metal removal by elevating the $Fe(II)$ regeneration.

In this study, $Cr(VI)$ was chosen as a typical heavy metal to explore the feasibility of the performance improvement of mZVI with the aid of boron powder. Firstly, we compared the removal performance of ZVI for $Cr(VI)$ with or without the addition of boron powder. Then, X-ray photoelectron spectroscopy (XPS) was utilized to reveal the variation of boron powder and ZVI, and an electrochemical method was applied to investigate the possible mechanism to explain the removal performance of the promoted $Cr(VI)$. Finally, in this study, we propose the possible enhancing mechanism of $Cr(VI)$ removal with boron powder.

2. Materials and methods

2.1 Chemicals

Microscale ZVI powder (100 mesh) was obtained from Shanghai Macklin Biochemical Co., Ltd. Ferric chloride hexahydrate ($FeCl_3 \cdot 6H_2O$), hydroxylamine hydrochloride ($HONH_2HCl$), sodium acetate (CH_3COONa), 1,10-phenanthroline, hydrochloric acid (HCl), boron trioxide (B_2O_3), boric acid (H_3BO_3), amorphous boron powder (B), iron(III) nitrate nonahydrate, and sodium nitrate were supplied by Sinopharm Chemical Reagents Co., Ltd.

2.2 Pretreatment method of mZVI and boron powder

To reduce the iron oxide layer on the surface of the mZVI powder, 2 g of commercial mZVI powder was placed in 20 mL of HCl solution (1 mol L^{-1}) for 2 min. Subsequently, deionized water and ethanol were utilized to wash the soaked mZVI powder. Then, the treated mZVI powder was dried at approximately 80 °C using argon (Ar) as the protection gas to avoid the oxidation of mZVI. To reveal the effect of boron valency on $Cr(VI)$ removal efficiency, amorphous boron powder was annealed in a muffle furnace for six hours at 400 °C in the air to functionalize the surface through partial oxidation, and the treated powder was named Boron-400.

2.3 Cr(VI) removal experiments

$Cr(VI)$ removal experiments were conducted in an Erlenmeyer flask (100 mL). Typically, 0.05 g of mZVI and 0.005 g boron powder were added to 50 mL of $Cr(VI)$ solution (1 mg L^{-1}) to start the reaction at room temperature (~25 °C) without pH adjustment. During the experiment, 1 mL suspension was taken out at periodic intervals with a syringe and filtered through a syringe filter (0.22 μm) for the next concentration analysis. The initial

pH values were adjusted with HCl (1 mol L^{-1}) and NaOH (1 mol L^{-1}) solution. To reveal the effect of dissolved oxygen on $Cr(VI)$ removal, anaerobic $Cr(VI)$ removal experiments were conducted in a three-necked flask using Ar to isolate oxygen. All experiments were performed in duplicates.

2.4 Analytical methods

The $Cr(VI)$ concentration was analyzed by the 1,5-diphenylcarbazide colorimetric method, and the dissolved iron ions concentration was detected by the 1,10-phenanthroline method.[30] The absorbance of $Cr(VI)$-1,5-diphenylcarbazide and $Fe(II)$-1,10-phenanthroline complexes were monitored at 540 nm and 510 nm. The concentration of the dissolved boron was detected using an Agilent 8900x triple quadrupole ICP-MS. The concentration of total chromium was monitored by flame atomic absorption spectrum (AAS, iCE3300, Thermo Fisher).

2.5 Electrochemical analysis tests

Cyclic voltammetry (CV) tests were performed in a two-electrode system, which comprised a saturated calomel reference-electrode, and a platinum plate as an auxiliary electrode (10 mm × 10 mm). An electrochemical workstation (CHI 660E) was used to accomplish testing requirements. In brief, a 20 mL electrolyte solution (pH 3.0) was prepared with 0.2 mmol L^{-1} iron(III) nitrate nonahydrate and 0.05 mol L^{-1} sodium nitrate. Then, CV scans were recorded at a scanning rate of 5 mV s^{-1} between −0.5 V and +1.5 V.

2.6 Characterization of mZVI and boron

Scanning electron microscopy (SEM) images were analyzed with TESCAN MIRA LMS. X-ray diffraction (XRD) patterns were collected to analyze the crystalline structure of mZVI and boron with a Bruker D2 PHASER (Germany) instrument. XPS spectra were monitored using the Thermo Scientific ESCALAB 250Xi instrument at 15 kV and 10 mA. To correct the binding energy of XPS spectra, the C (1s) peak of an aliphatic indefinite hydrocarbon at 284.8 eV was utilized.

3. Results and discussion

3.1 Characterization of mZVI and boron

As shown in Fig. 1a–d, the SEM images of mZVI and boron powder were composed of irregular particles, and their surfaces were uneven with grooves.

Subsequently, XRD was utilized to analyze the crystalline structure of mZVI and boron. As shown in Fig. 2, the XRD pattern of mZVI matched well with that of iron (JCPDS file no. 06-0696). The weak peak intensity attributed to boron powder (JCPDS file no. 71-0157) suggested the low degree of crystallinity of boron powder used in this study.

3.2 Cr(VI) removal with mZVI and boron

Subsequently, in this study, we compared the $Cr(VI)$ removal efficiency with boron or mZVI in the presence or absence of boron. As exhibited in Fig. 3a, the $Cr(VI)$ removal percentage
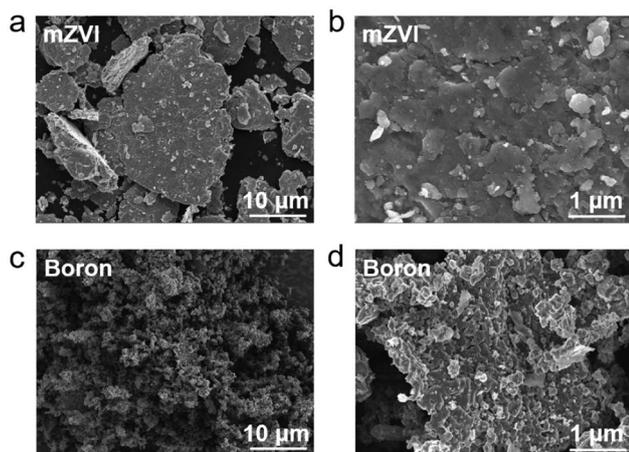
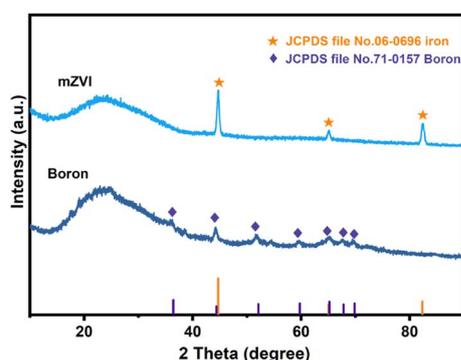Fig. 1 SEM images of (a and b) mZVI and (c and d) boron.

Fig. 2 XRD patterns of mZVI and boron.

with boron only reached 10% within 240 min, and mZVI without boron powder could remove 95% of Cr(VI). In contrast, the addition of mZVI and boron powder exhibited superior reactivity and removed 100% of Cr(VI) within 240 min, suggesting that boron powder could promote the reactivity of mZVI for Cr(VI) removal. Furthermore, Cr(VI) removal kinetic analysis indicated that the Cr(VI) removal process obeyed the pseudo-first-order kinetic equation, and the apparent Cr(VI) removal rate constant with boron powder was only 6.30×10^{-4} min^{-1} (Fig. 3b). The presence of boron powder promoted the apparent Cr(VI) removal rate constant with mZVI from 1.11×10^{-2} to 2.33×10^{-2} min^{-1}, further demonstrating that boron powder indeed enhanced the Cr(VI) removal efficiency. Subsequently, we utilized AAS to monitor the residual total chromium concentration. It was found that the residual total chromium concentrations were 6.67×10^{-3} and 1.69×10^{-2} mg L^{-1} with mZVI in the presence and absence of boron powder, respectively (Fig. 3c). Most of the Cr(VI) was reduced to Cr(III), and Cr(III) can be deposited on the surface of mZVI, and then separated from the solution to achieve the removal. Therefore, boron could not only enhance the reactivity of mZVI for the Cr(VI) removal percentage, but also the total chromium pollution remediation. Since the pH value would significantly affect the reactivity of

mZVI, we further monitored the pH value variation during the Cr(VI) removal process. As shown in Fig. 3d, the pH values in all systems rose slightly at first 20 min and then stabilized approximately at 5.7–6.0. This result indicated that it was not the differences in the pH value that caused the difference in the Cr(VI) removal efficiency.

3.3 Effect of initial pH value and dissolved oxygen on Cr(VI) removal

Subsequently, the effect of initial pH value on the performance of Cr(VI) removal by mZVI with or without boron was investigated. As exhibited in Fig. 4a, the Cr(VI) removal percentage by mZVI in the presence or absence of boron under acidic conditions was considerably higher than that in an alkaline pH environment because of the inhibited corrosion rate of mZVI under alkaline conditions, and the presence of boron could weaken the reduction effect of alkaline environment for Cr(VI) removal with mZVI. Apart from the initial pH value, dissolved oxygen is also a crucial environmental factor for the mZVI performance. To illustrate the effect of dissolved oxygen on Cr(VI) removal efficiency by mZVI in the presence of boron, we compared Cr(VI) removal curves *versus* time in the mZVI/boron system under air and Ar atmospheres and found that the Cr(VI) removal efficiency without dissolved oxygen was remarkably higher than that under air atmosphere due to the lack of electron competitors (Fig. 4b). Moreover, the apparent reaction rate constant under Ar condition (4.31×10^{-2} min^{-1}) was 1.85 times that under air condition (2.33×10^{-2} min^{-1}) (Fig. 4c), revealing that the reduction pathway was involved during the Cr(VI) removal process.

3.4 Cyclic experiments of mZVI and boron

We conducted the cyclic experiments of Cr(VI) removal with mZVI in the presence and absence of boron, and the results are exhibited in Fig. 5. It was found that the Cr(VI) removal percentage would be decreased with the increase in time with or without boron powder. In fact, the mZVI would be oxidized during the Cr(VI) removal process; therefore, it was difficult to achieve excellent cyclic performance for mZVI.

3.5 Enhanced mechanism of Cr(VI) removal with mZVI and boron

In general, Cr(VI) could be removed *via* two pathways, including adsorption and reduction. To reveal the main promoted mechanism of Cr(VI) removal with mZVI in the presence of boron, XPS was used to evaluate the valence of the chromium element on the surface of mZVI samples after the reaction. As shown in Fig. 6, both Cr(III) and Cr(VI) appeared on the surface of mZVI with or without the addition of boron after the reaction,[31] illustrating that both the reduction and adsorption mechanisms were included during the Cr(VI) removal process. Furthermore, we analyzed the ratio of Cr(VI) and Cr(III) after the reaction and found that the presence of boron promoted the Cr(III) proportion from 79.4% to 84.2%, revealing that boron might enhance the performance of mZVI for the Cr(VI) removal *via* the reduction mechanism.
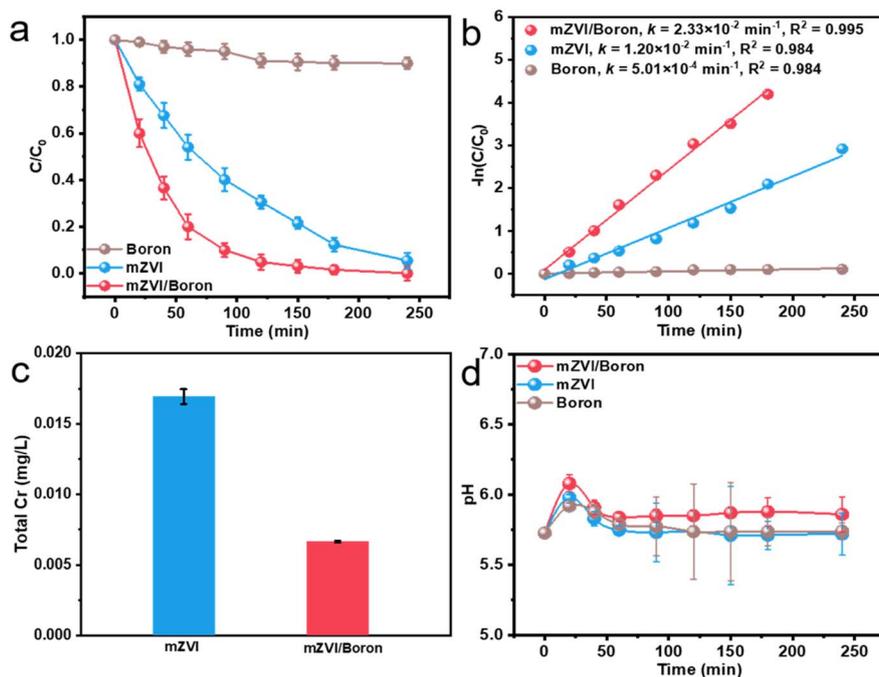
Fig. 3 (a) Cr(VI) removal with boron or mZVI in the presence or absence of boron powder; (b) kinetic analysis of Cr(VI) removal with boron or mZVI in the presence or absence of boron powder; (c) total chromium concentration after the treatment of mZVI in the presence or absence of boron powder; (d) variation of pH values during the Cr(VI) removal process by boron or mZVI in the presence or absence of boron powder.
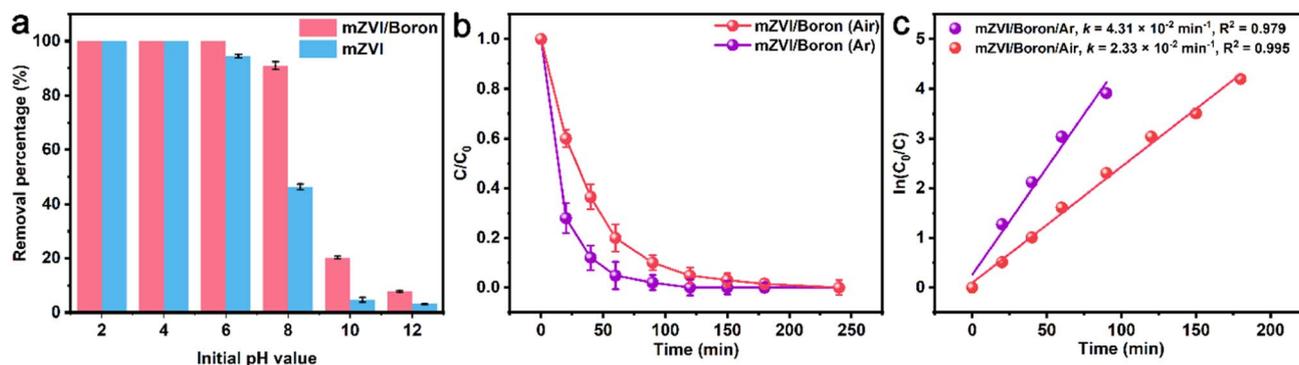

Fig. 4 (a) Cr(VI) removal percentage with mZVI in the presence and absence of boron at different initial pH values; (b) Cr(VI) removal curves *versus* time with mZVI and boron in air and Ar atmospheres; (c) pseudo-first-order kinetic fitting curves of Cr(VI) removal with mZVI and boron in air and Ar atmospheres.

Generally, the main species of mZVI for the Cr(VI) reduction process included electrons released by the iron core and ferrous ions accompanied by the corrosion process of mZVI. Considering that previous studies have revealed that boron with reduction ability could promote the iron cycle process from Fe(III) to Fe(II),[21,22] we supposed that the enhanced Cr(VI) reduction process could be attributed to the promoted Fe(III) reduction and Fe(II) regeneration. To verify the above hypothesis, we further compared the Cr(VI) removal efficiency of Fe(III) with or without the addition of boron. As exhibited in Fig. 7a, only 10.1% of Cr(VI) removal percentage was accomplished with Fe(III), and boron could only remove 1.55% of Cr(VI) within 240 min. In contrast, the presence of Fe(III) and boron led to 33.6% removal

of Cr(VI), indicating that boron might promote the efficiency of Cr(VI) removal by enhancing the reduction of Fe(III) to Fe(II) during the Cr(VI) removal process with mZVI in the presence of boron. To confirm the enhanced mechanism of boron, in this study, we analyzed the differences between the oxidation and reduction potential of Fe(III) with or without boron. Firstly, we monitored the cyclic voltammetry curve of the boron powder in sodium nitrate solution, and no significant oxidation or reduction potential peak was found (Fig. 7b), suggesting the high stability of boron. Subsequently, we observed the oxidation and reduction potential of Fe(III) with or without the addition of boron. As shown in Fig. 7c, the gap values (ΔE_p) between Fe(III) reduction and Fe(II) oxidation with or without boron were 0.556 V
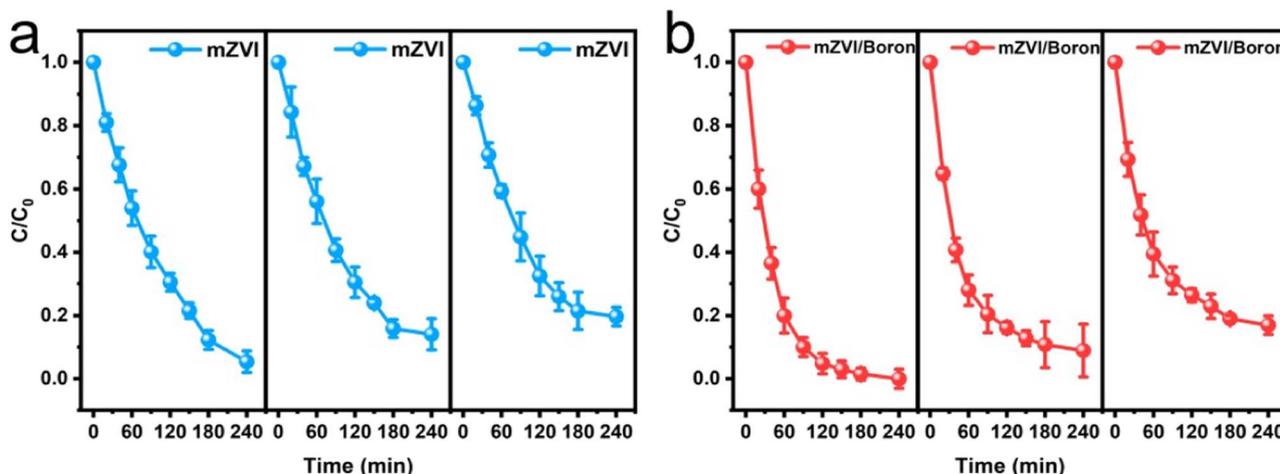
Fig. 5 (a) Cyclic experiments of mZVI in the absence of boron for Cr(VI) removal; (b) cyclic experiments of mZVI in the presence of boron for Cr(VI) removal.
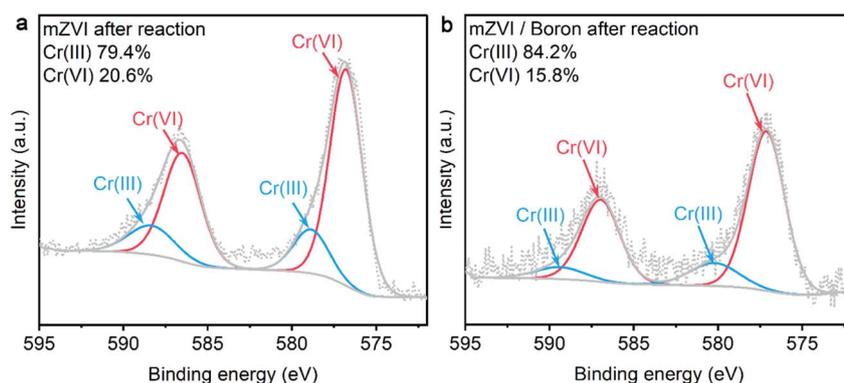

Fig. 6 High-resolution XPS spectra of Cr 2p on the surface of the sample after reaction: (a) sample after reaction in the mZVI system; (b) sample after reaction in the mZVI/boron system.

and 0.668 V, respectively. This result further revealed that the presence of boron could accelerate Fe(II) regeneration and promote the Cr(VI) reduction process with Fe(II).

Considering that our results revealed that boron powder would act as a reductant to promote the iron cycle, thus enhancing the Cr(VI) reduction process, and therefore oxidizing

the boron powder, we further utilized XPS to analyze the valence variation of boron element on the boron powder before and after the reaction. As shown in Fig. 8, boron powder before and after the reaction exhibited three kinds of states, including B–B around 186.7 eV, suboxide boron around 188.5 eV, and boron oxide (B–O) at 192.1 eV.[20] Meanwhile, the B–B ratio increased
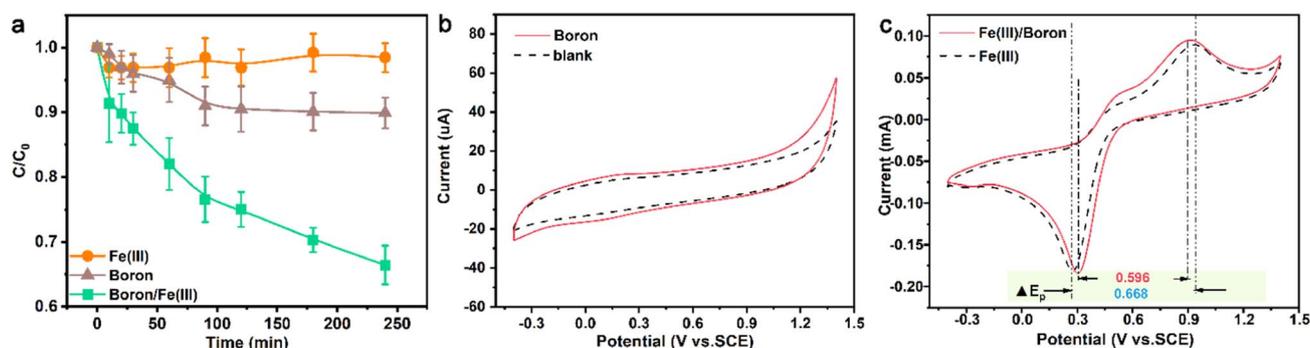

Fig. 7 (a) The Cr(VI) removal curves with Fe(III) in the presence and absence of boron; (b) CV scan curves in sodium nitrate solution (blank) and electrolyte with boron monomer; (c) CV scan curves for Fe(III) in the presence or absence of boron monomer.
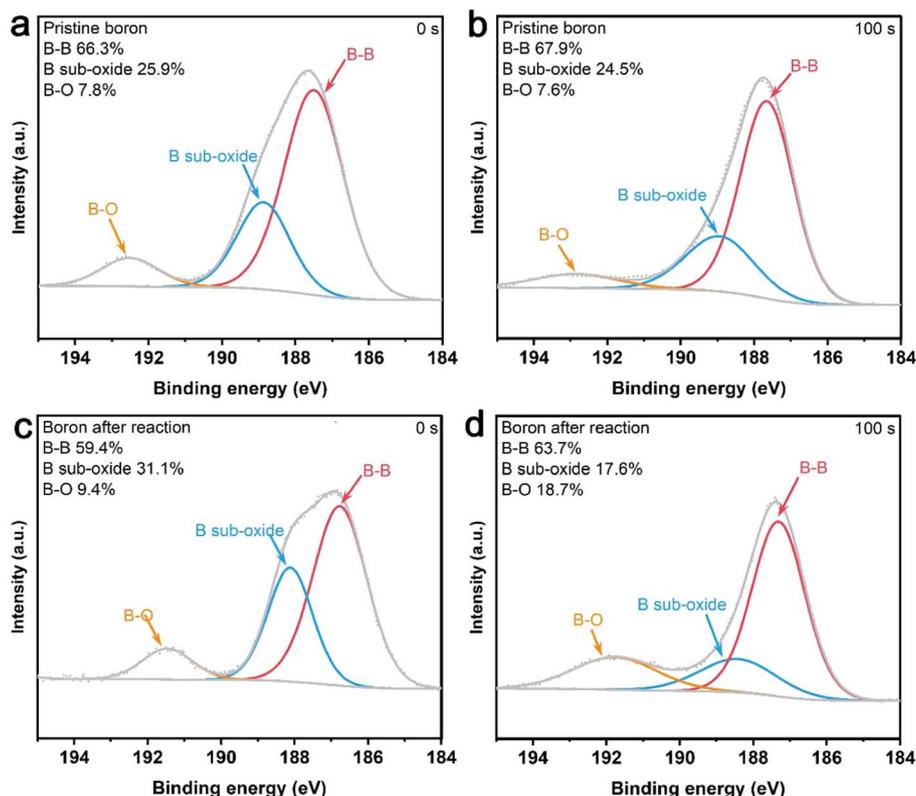
Fig. 8 High-resolution XPS spectrum of B 1s for boron powder before and after the reaction with different etching times: (a) boron powder before reaction without etching; (b) boron powder before reaction with 100 s of etching; (c) boron powder after reaction without etching; (d) boron powder after reaction with 100 s of etching.

slightly from 66.3% to 67.9% with the increase of etching time from 0 s to 100 s, suggesting that boron on the surface of boron powder exhibited a higher degree of oxidation.

The XPS results demonstrated that boron powder would be oxidized during the Cr(VI) removal process. To further reveal if the removal performance of the promoted Cr(VI) was caused by the dissolved boric acid or the generated boron oxide, we monitored the total dissolved boron concentration and compared the Cr(VI) removal efficiency with mZVI in the presence of boric acid or boron oxide. As shown in Fig. 9a, the

concentration of boron in the presence of mZVI was 2.15 mg L^{-1}, which was 1.99 times that in the absence of mZVI. Subsequently, the Cr(VI) removal with mZVI and boric acid, boron oxide, or boron powder treated at 400 °C in air were compared, and results indicated that both boric acid and boron oxide would significantly inhibit the percentage of Cr(VI) removal with mZVI. However, boron powder treated at 400 °C in air suppressed Cr(VI) removal in 90 min, and then enhanced the Cr(VI) removal efficiency (Fig. 9b), which might be attributed to the dissolution of boron oxide on the surface and exposure of
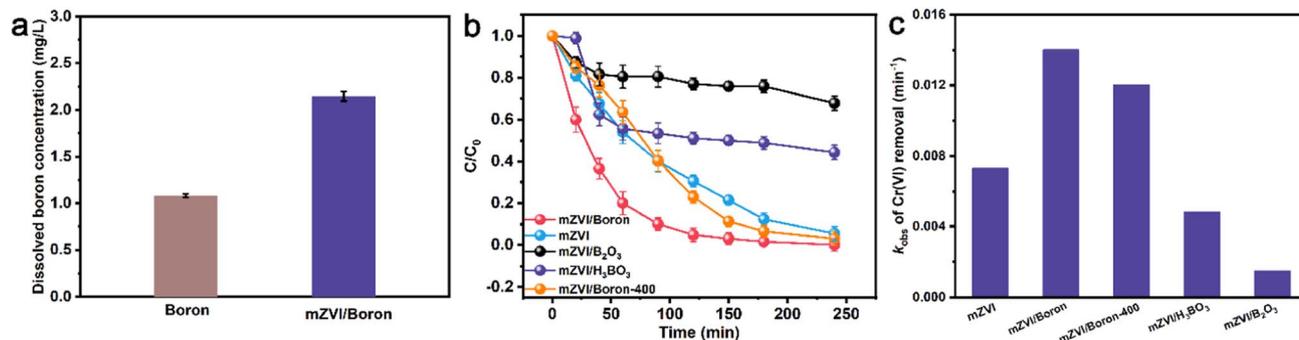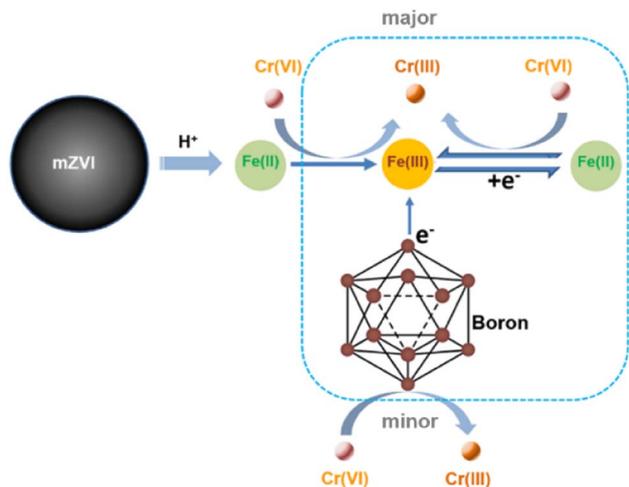

Fig. 9 (a) Dissolved boron concentration after the reaction in the mZVI and mZVI/boron system; (b) Cr(VI) removal performance of mZVI with the addition of boron powder, boric acid, boron oxide, or boron powder treated at 400 °C in air; (c) apparent Cr(VI) removal rate of mZVI with the addition of boron powder, boric acid, boron oxide, or boron powder treated at 400 °C in air.

Scheme 1 Possible enhanced mechanism of Cr(VI) removal with boron powder and mZVI.

new surfaces in the inner boron. The higher rate constant of Cr(VI) removal suggested that boron and that treated at 400 °C in air promoted Cr(VI) removal rate, and boric acid and boron oxide inhibited the Cr(VI) removal rate (Fig. 9c). The above results further demonstrated that boron with oxidized valence would not promote the performance of mZVI.

4. Conclusions

In this study, we found that the Cr(VI) removal rate by mZVI and boron powder was enhanced 2.1 times without the addition of boron powder. Generally, the removal of Cr(VI) with mZVI involved reduction and adsorption pathways. The added boron powder could act as an electron sacrificial agent to promote the reduction process of Fe(III) to Fe(II), and thus enhance the reduction of Cr(VI) with Fe(II). The possible enhancement for the Cr(VI) removal mechanism of boron powder with mZVI is proposed in Scheme 1. In summary, this study provided a theoretically feasible approach to promote the reactivity of mZVI by accelerating the iron cycle process, which would favor the wide application of mZVI technology in the environmental remediation field.

Author contributions

Wenjuan Shen: writing – review and editing, conceptualization, supervision. Yan Gao: investigation, formal analysis, methodology, writing – original draft. Zhan Liu: investigation, methodology. Xu Zhang: investigation, methodology. Fengjiao Quan: validation. Xing Peng: funding acquisition, conceptualization. Xiaobing Wang: investigation. Jianfen Li: funding acquisition. Zhenhua Qin: methodology, data curation. Yun He: investigation. Hui Li: investigation.

Conflicts of interest

There are no conflicts to declare.

Acknowledgements

References

1 W. Sun, S. Wang, Z. Yu and X. Cao, Characteristics and application of iron-based materials in heterogeneous Fenton oxidation for wastewater treatment: a review, *Environ. Sci.: Water Res. Technol.*, 2023, **9**, 1266–1289.

2 W. Shen, Z. Liu, F. Quan, X. Zhang, X. Peng, X. Wang, W. Wang, L. Huang, S. Zhang, J. Li and Y. Mei, Mechanochemically activated microscale zero-valent iron with carboxymethylcellulose for efficient sequestration of phosphate in aqueous solution, *J. Environ. Chem. Eng.*, 2023, **11**, 109066.

3 S. Li, W. Wang, F. Liang and W.-x. Zhang, Heavy metal removal using nanoscale zero-valent iron (nZVI): theory and application, *J. Hazard. Mater.*, 2017, **322**, 163–171.

4 S. Guo, H. Yang, Q. Sun, G. Zhang, T. Zhao, Y. Zhou, X. Li and P. Gao, Evaluation of a novel carbon-based micro-nano zero-valent iron composite for immobilization of heavy metals in soil, *J. Environ. Chem. Eng.*, 2023, **11**, 109740.

5 K. Terzi, A. Sikinioti-Lock, A. Gkelios, D. Tzavara, A. Skouras, C. Aggelopoulos, P. Klepetsanis, S. Antimisiaris and C. D. Tsakiroglou, Mobility of zero valent iron nanoparticles and liposomes in porous media, *Colloids Surf., A*, 2016, **506**, 711–722.

6 Z. H. Farooqi, R. Begum, K. Naseem, W. Wu and A. Irfan, Zero valent iron nanoparticles as sustainable nanocatalysts for reduction reactions, *Catal. Rev.*, 2022, **64**, 286–355.

7 H. L. Lien and R. T. Wilkin, High-level arsenite removal from groundwater by zero-valent iron, *Chemosphere*, 2005, **59**, 377–386.

8 S. Comba, A. Di Molfetta and R. Sethi, A comparison between field applications of nano-, micro-, and millimetric zero-valent iron for the remediation of contaminated aquifers, *Water, Air, Soil Pollut.*, 2011, **215**, 595–607.

9 P. D. Mines, B. Uthuppu, D. Thirion, M. H. Jakobsen, C. T. Yavuz, H. R. Andersen and Y. Hwang, Granular activated carbon with grafted nanoporous polymer enhances nanoscale zero-valent iron impregnation and water contaminant removal, *Chem. Eng. J.*, 2018, **339**, 22–31.

10 Y. Mu, F. Jia, Z. Ai and L. Zhang, Iron oxide shell mediated environmental remediation properties of nano zero-valent iron, *Environ. Sci.: Nano*, 2017, **4**, 27–45.

11 L. Gong and L. Zhang, Oxyanion-modified zero valent iron with excellent pollutant removal performance, *Chem. Commun.*, 2023, **59**, 2081–2089.

12 M. Liao, S. Zhao, K. Wei, H. Sun and L. Zhang, Precise decomplexation of Cr(III)-EDTA and in-situ Cr(III) removal

with oxalated zero-valent iron, *Appl. Catal., B*, 2023, **330**, 122619.

13 K. Wei, H. Li, H. Gu, X. Liu, C. Ling, S. Cao, M. Li, M. Liao, X. Peng, Y. Shi, W. Shen, C. Liang, Z. Ai and L. Zhang, Strained zero-valent iron for highly efficient heavy metal removal, *Adv. Funct. Mater.*, 2022, **32**, 2200498.

14 X. Zhang, H. Sun, Y. Shi, C. Ling, M. Li, C. Liang, F. Jia, X. Liu, L. Zhang and Z. Ai, Oxalated zero valent iron enables highly efficient heterogeneous Fenton reaction by self-adapting pH and accelerating proton cycle, *Water Res.*, 2023, **235**, 119828.

15 W. Shen, X. Wang, F. Jia, Z. Tong, H. Sun, X. Wang, F. Song, Z. Ai, L. Zhang and B. Chai, Amorphization enables highly efficient anaerobic thiamphenicol reduction by zero-valent iron, *Appl. Catal., B*, 2020, **264**, 118550.

16 C. Liu, B. Wu and X. e. Chen, Ultrasound enhanced zero-valent iron-activated peroxymonosulfate oxidation for improving dewaterability of aerobically digested sludge, *Chem. Eng. J.*, 2020, **392**, 124850.

17 J. Zhao, A. Su, P. Tian, X. Tang, R. N. Collins and F. He, Arsenic (III) removal by mechanochemically sulfidated microscale zero valent iron under anoxic and oxic conditions, *Water Res.*, 2021, **198**, 117132.

18 L. Liang, W. Sun, X. Guan, Y. Huang, W. Choi, H. Bao, L. Li and Z. Jiang, Weak magnetic field significantly enhances selenite removal kinetics by zero valent iron, *Water Res.*, 2014, **49**, 371–380.

19 C. C. Huang and H. L. Lien, Trimetallic Pd/Fe/Al particles for catalytic dechlorination of chlorinated organic contaminants, *Water Sci. Technol.*, 2010, **62**, 202–208.

20 P. Zhou, W. Ren, G. Nie, X. Li, X. Duan, Y. Zhang and S. Wang, Fast and long-lasting iron(III) reduction by boron toward green and accelerated Fenton chemistry, *Angew. Chem., Int. Ed.*, 2020, **59**, 16517–16526.

21 P. Zhou, S. Meng, M. Sun, K. Hu, Y. Yang, B. Lai, S. Wang and X. Duan, Insights into boron accelerated Fenton-like chemistry: sustainable and fast Fe^{III}/Fe^{II} circulation, *Sep. Purif. Technol.*, 2023, **317**, 123860.

22 C. W. Yuan, C. W. Bai, K. A. Zhu, X. J. Chen, Y. J. Sun, B. B. Zhang, Q. Yang and F. Chen, Metal-free boron-assisted Fe(III)/peracetic acid system for ultrafast removal of organic contaminants: Role of crystalline nature and interfacial suboxide boron intermediates, *Chem. Eng. J.*, 2023, **454**, 140049.

23 P. Zhou, F. Cheng, G. Nie, Y. Yang, K. Hu, X. Duan, Y. Zhang and S. Wang, Boron carbide boosted Fenton-like oxidation: a novel Fe(III)/Fe(II) circulation, *Green Energy Environ.*, 2020, **5**, 414–422.

24 Y. Zhang, P. Zhou, R. Huang, C. Zhou, Y. Liu, H. Zhang, X. Huo, J. Zhao, Z. Xiong and B. Lai, Iron boride boosted Fenton oxidation: Boron species induced sustainable Fe^{III}/Fe^{II} redox couple, *J. Hazard. Mater.*, 2023, **443**, 130386.

25 S. Meng, M. Sun, P. Zhang, C. Zhou, C. He, H. Zhang, Y. Liu, Z. Xiong, P. Zhou and B. Lai, Metal borides as excellent Co-catalysts for boosted and long-lasting Fenton-like reaction: dual Co-catalytic centers of metal and boron, *Environ. Sci. Technol.*, 2023, **57**, 12534–12545.

26 P. Zhou, Y. Yang, W. Ren, X. Li, Y. Zhang, B. Lai, S. Wang and X. Duan, Molecular and kinetic insights to boron boosted Fenton-like activation of peroxymonosulfate for water decontamination, *Appl. Catal., B*, 2022, **319**, 121916.

27 Z. Zhou, J. Huang, M. Danish, G. Zeng, R. Yang, X. Gu, M. Ali and S. Lyu, Insights into enhanced removal of 1,2-dichloroethane by amorphous boron-enhanced Fenton system: Performances and mechanisms, *J. Hazard. Mater.*, 2021, **420**, 126589.

28 W. Chen, X. Xu, J. Cui, Z. Zhou and Y. Yao, Porous boron nitride intercalated zero-valent iron particles for highly efficient elimination of organic contaminants and Cr (VI), *Chemosphere*, 2022, **306**, 135501.

29 U. Lawal Usman, B. Kumar Allam, N. Bahadur Singh and S. Banerjee, Adsorptive removal of Cr(VI) from wastewater by hexagonal boron nitride-magnetite nanocomposites: Kinetics, mechanism and LCA analysis, *J. Mol. Liq.*, 2022, **354**, 118833.

30 A. E. Harvey Jr, J. A. Smart and E. S. Amis, Simultaneous spectrophotometric determination of iron(II) and total Iron with 1,10-phenanthroline, *Anal. Chem.*, 1955, **27**, 26–29.

31 Y. Mu, Z. Ai, L. Zhang and F. Song, Insight into core–shell dependent anoxic Cr(VI) removal with $Fe@Fe_2O_3$ nanowires: indispensable role of surface bound Fe(II), *ACS Appl. Mater. Interfaces*, 2015, **7**, 1997–2005.